

Tunable VO₂/Au hyperbolic metamaterial

S. Prayakarao¹, B. Mendoza^{2,3}, A. Devine^{2,3}, C. Kyaw², R. B. Van Dover², V. Liberman⁴, M. A. Noginov^{1*}

¹Center for Materials Research, Norfolk State University, Norfolk, VA 23504, USA

²Summer Research Program, Center for Materials Research, Norfolk State University, Norfolk, VA 23504, USA

³Materials Science and Engineering Department, Cornell University, Ithaca, New York 14850, USA

⁴MIT LINCOLN Laboratory, 244 Wood Street, Lexington, Massachusetts 02420, USA

Distribution A: Public Release

*mnoginov@nsu.edu

Abstract

Vanadium dioxide (VO₂) is known to have a semiconductor-to-metal phase transition at ~68°C. Therefore, it can be used as a tunable component of an active metamaterial. The lamellar metamaterial studied in this work is composed of subwavelength VO₂ and Au layers and designed to undergo the temperature controlled transition from the *optical* hyperbolic phase to the metallic phase. The VO₂ films and VO₂/Au lamellar metamaterial stacks have been fabricated and studied in the electrical conductivity and optical (transmission and reflection) experiments. The observed temperature dependent changes in the reflection and the transmission spectra of the metamaterials and VO₂ thin films are in a good qualitative agreement with the theoretical predictions. The demonstrated optical hyperbolic-to-metallic phase transition is a novel physical phenomenon having a potential of advancing the control of light-matter interaction.

Metamaterials are engineered composite materials containing sub-wavelength inclusions with rationally designed shapes, sizes, mutual arrangements and orientations¹⁻⁴. They enable unmatched control of light wave propagation, feature scores of unique properties, including negative index of refraction⁵⁻⁷, and lead to unparalleled applications ranging from sub-wavelength imaging and focusing^{8,9} to optical cloaking¹⁰ and future nanocircuitry operating at optical frequencies¹¹. Recently, a special class of metamaterials known as *hyperbolic metamaterials* has attracted much attention¹²⁻¹⁵. In these materials, the dielectric permittivity components in orthogonal directions have opposite signs. Consequently, the iso-frequency dispersion surfaces (for extraordinary waves) form hyperboloids rather than ellipsoids¹⁵ – the phenomenon known as *hyperbolic dispersion*. Hyperbolic metamaterials can propagate light waves with very large wave vectors and have a broadband singularity of the photonic density of states¹⁶. The latter property makes these materials highly efficient absorbers¹⁷ and allows them to control the rate, the spectra, and the directionality of spontaneous emission^{16,18-21}.

One of the most common designs of hyperbolic metamaterials is based on lamellar stacks of metallic and dielectric layers. The optical properties of such metamaterials can be tuned *passively* by selecting constituent material components with optimized dielectric permittivities or changing the metal filling factor during fabrication. At the same time, many applications require *active* metamaterials, whose properties can be tuned by external stimuli. In this work, we develop a tunable metamaterial that can undergo temperature induced reversible transitions between hyperbolic and metallic *optical* phases.

*The Lincoln Laboratory portion of this work was sponsored by the Assistant Secretary of Defense for Research & Engineering under Air Force Contract No. FA8721-05-C-0002. Opinions, interpretations, conclusions, and recommendations are those of the authors and are not necessarily endorsed by the United States Government.

Some transition metal oxides are known to have the semiconductor-to-metal phase transition²². Particularly, vanadium dioxide (VO_2) undergoes the phase transition at 68°C ²³ that can be induced by heat or laser pulse²⁴. At room temperature, VO_2 is a semiconductor with the monoclinic crystal structure. When heated past the phase transition temperature, the material changes its structure to obtain the tetragonal rutile crystal symmetry and acts as a metal. This structural transformation is accompanied by strong changes in the electrical and optical properties. Thus, the phase transition in VO_2 has been used in ultrafast switches and sensors²⁵, reversible tunable plasmonic nanostructures²⁶, optical memory²⁷ as well as tunable metamaterials^{28, 29}. In particular, in Ref. 29 VO_2 was used as a component of a lamellar VO_2/TiO_2 metamaterial that could be tuned by temperature from the elliptical dispersion phase to a hyperbolic dispersion phase. In this work, we have fabricated and studied the new type of active metamaterial, based on VO_2/Au lamellar stacks, whose optical dispersion phase can be changed from hyperbolic to anisotropic metallic.

Both VO_2 thin films and lamellar VO_2/Au metamaterials have been fabricated using the pulsed laser deposition (PLD) technique (Neocera Ex200 apparatus). The KrF excimer laser operating at $\lambda=248$ nm and 10 Hz repetition rate was focused onto a target – vanadium metal or gold metal (99.99% purity). All samples were grown on the (300) and (012) sapphire substrates. The deposition chamber was pumped to $< 10^{-6}$ Torr before introducing oxygen gas. The depositions were performed at 1 mTorr to 30 mTorr of oxygen and the substrate temperature was maintained between $600 - 900^\circ\text{C}$. The properties of the VO_2 thin films and lamellar VO_2/Au metamaterial strongly depended on the substrate temperature and oxygen pressure during the deposition. The films, which exhibited the most pronounced semiconductor-to-metal transition (as discussed below), were deposited at the temperatures ranging between 600°C and 900°C at the oxygen pressure equal to 30 mTorr. The thickness of the VO_2 thin films, which were not a part of the metamaterial (determined by using the DekTak XT profilometer or ellipsometry, as described below), ranged between ~ 60 nm and ~ 190 nm. At the same time, the thicknesses of VO_2 and Au layers composing lamellar VO_2/Au metamaterial, determined by using the MicroXAM optical interferometric surface profiler, were equal to ~ 30 nm for VO_2 and ~ 20 nm for Au. The metamaterial samples studied consisted of six pairs of VO_2/Au with Au on top or VO_2 on top, as shown in Fig. 1.

In the experiments, the samples were mounted on top of the metal ceramic heater with 4 mm hole in the center, allowing for the transmission measurements, as shown in Fig. 1. The temperature was measured using the 10 kOhm thermistor, and both the current and the temperature were regulated using TC200 controller (all from Thorlabs).

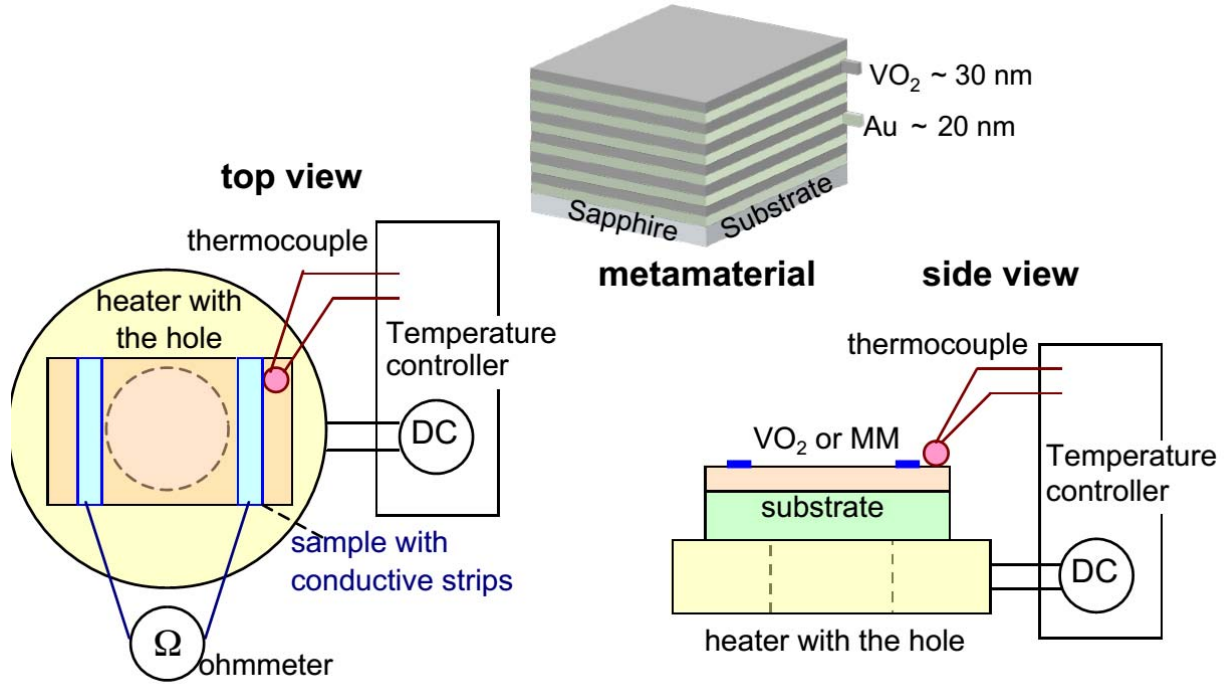


FIG. 1. Schematic of the metamaterial and the sample mounted on the heater (top view and side view).

The electrical resistance R of the elongated nearly rectangular VO₂ thin film samples has been studied in the two-contact scheme using a precision multimeter (Fig. 2). The resistivity ρ was estimated knowing the resistance R and the geometry of the film (width, thickness and the distance between the contacts). As one can see in Fig. 3(a), depicting the temperature dependence $\rho(T)$, as the temperature increased from 300 K to 360 K, (i) the resistivity dropped by approximately thousand times, (ii) the temperature range of the phase transition (change of the resistivity from high to low) was of the order of 30°C, and (iii) the $\rho(T)$ curve had mild hysteresis. The magnitude of the resistivity drop and the hysteresis were consistent with those described in the literature³⁰, while the temperature range of the phase transition in our experiment was somewhat larger, Fig. 2.

The transmittance and reflectance spectra of the VO₂ thin films and lamellar metamaterials were measured using the Lambda 900 spectrophotometer equipped with an integrating sphere (Perkin Elmer) and the homemade heater described above. In the transmission measurements, the samples were installed at the entrance port of the integrating sphere, oriented normally to the incident light beam. In the reflectance studies, the samples were installed at the exit port of the integrating sphere at the incidence angle equal to 8 degrees.

As the temperature was increased from 29 °C to 69 °C and the VO₂ film passed through the semiconductor-to-metal phase transition, a dramatic decrease in the transmission (which reduced monotonically with increase of the temperature) has been observed in the infrared spectral range, while no significant change was detected in the visible part of the spectrum (Fig. 3(a)). At the same time, the sample's reflectance showed a tendency to decrease, when the temperature was changed from 29 °C to 59 °C, and then increased sharply as the sample passed through the phase

transition at $\sim 69^\circ\text{C}$ (Fig. 3(b)). This behavior of both transmittance and reflectance is expected of the semiconductor-to-metal transition, where the real part of dielectric permittivity changes gradually from positive to negative values.

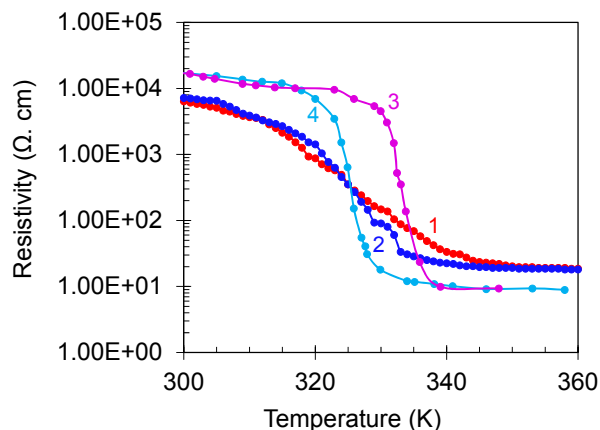


FIG. 2. Resistivity of the fabricated VO_2 sample measured at slow increase (trace 1, red) and slow reduction (trace 2, blue) of the temperature. Temperature dependence of the VO_2 resistivity reported in Ref. 30 at increase (trace 3, pink) and reduction (trace 4, light blue) of the temperature.

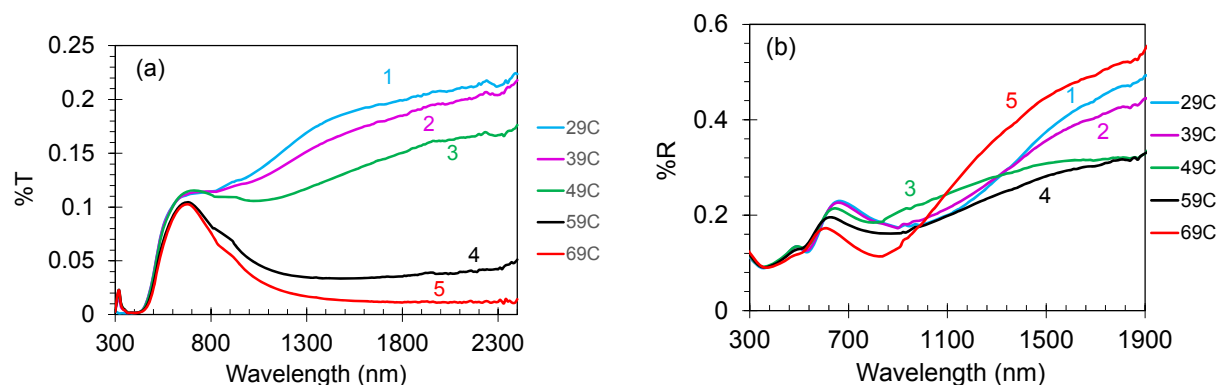


FIG. 3. Transmittance (a) and reflectance (b) spectra of the VO_2 thin film at the temperatures below (traces 1 and 2), around (traces 3 and 4), and above (trace 5) the phase transition temperature. (The thickness of the VO_2 film, determined using ellipsometry, was equal to 63 nm.)

The dielectric permittivity spectra of VO_2 thin films were obtained from spectroscopic ellipsometry. Ellipsometric measurements were carried out using a Woollam M2000 spectroscopic ellipsometer, outfitted with a custom heating stage assembly. The heating stage can maintain a sample between room temperature and 100°C with 0.5°C temperature accuracy. Spectroscopic data was acquired at a specified temperature for a wavelength range 250 nm to 1000 nm and at seven angles of incidence between 45 degrees and 70 degrees. The beam spot for the instrument is 1 mm diameter at normal incidence. Refractive index and thickness of VO_2 thin films were extracted from ellipsometric data by using a Kramers-Kronig-consistent Tauc-Lorentz dispersion model³¹. Typically, four oscillators were used in the above model to obtain good quality fit over the full wavelength range. Once the dispersion model for the optical constants was obtained, we extrapolated the dielectric permittivity spectra beyond 1000 nm using the oscillator fit. The retrieved spectra of real ϵ' and imaginary ϵ'' parts of the dielectric permittivity

of the 63 nm thick VO₂ film in the semiconductor phase at 20 °C and the metallic phase at 84 °C are depicted in Fig. 4(a) and 4(b). The spectra of dielectric permittivity of VO₂ reported in the literature vary strongly from publication to publication [28, 32], and our experimental results are within the range of data reported in the literature. As one can see, the real part of dielectric permittivity ϵ' is positive (like in dielectrics) below the phase transition and is negative (at $\lambda > 1\mu\text{m}$, like in metals) at the temperature above the phase transition. This behavior correlates with the strong reduction of the dc electric resistivity (Fig. 2) and makes VO₂ highly attractive for both electronic and optical applications involving switching and tuning.

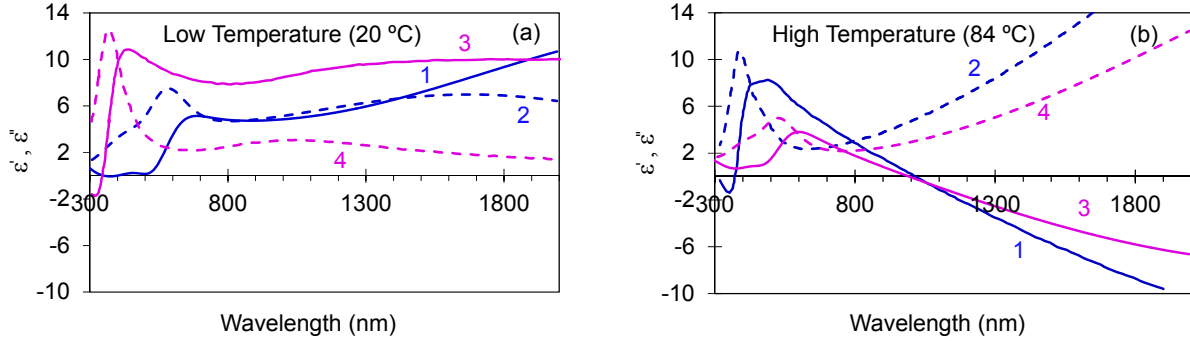


FIG. 4. Spectra of real ϵ' (traces 1 and 3) and imaginary ϵ'' (traces 2 and 4) parts of dielectric permittivity of the VO₂ thin film, determined using spectroscopic ellipsometry below the phase transition at 20 °C (a) and above the phase transition at 84 °C (b). Traces 1 and 2 –fabricated VO₂ sample (63 nm thick VO₂ film deposited on sapphire at 600 °C and 30 mTorr O₂); traces 3 and 4 – data reported in Ref. [32].

The dielectric permittivity of lamellar VO₂/Au metamaterial was modeled in the effective medium approximation^{33, 34}. The effective dielectric permittivity components in the directions parallel ϵ_{\parallel} and perpendicular ϵ_{\perp} to the layers, have been calculated as

$$\epsilon_{\parallel} = f\epsilon_{Au} + (1-f)\epsilon_{VO_2}$$

$$\frac{1}{\epsilon_{\perp}} = \frac{f}{\epsilon_{Au}} + \frac{(1-f)}{\epsilon_{VO_2}}, \quad (1)$$

where, ϵ_m and ϵ_d are the (complex) dielectric permittivities of Au and VO₂ and f is the filling factor of Au. The real and imaginary parts of the dielectric permittivities ϵ'_{\parallel} and ϵ'_{\perp} below and above the phase transition are depicted in Figs. 5(a) and 5(b), respectively. One can see that when VO₂ is in the semiconductor phase, the metamaterial is hyperbolic ($\epsilon'_{\perp} > 0$, $\epsilon'_{\parallel} < 0$) at $\lambda > 630$ nm, Fig. 5(a). However, when VO₂ changes its phase to metallic, the metamaterial is hyperbolic at $590 \text{ nm} < \lambda < 1000 \text{ nm}$ and anisotropic metallic ($\epsilon'_{\perp}, \epsilon'_{\parallel} < 0$) at $\lambda > 1000 \text{ nm}$, Fig. 5(b). Thus, by tuning the temperature, the metamaterial can be switched from the hyperbolic to the metallic optical phase at $\lambda > 1000 \text{ nm}$.

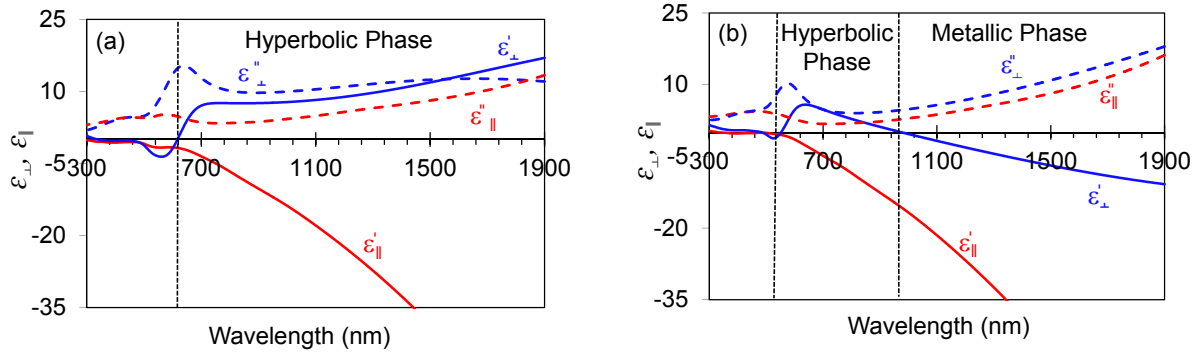


FIG. 5. Real (ϵ') and imaginary (ϵ'') parts of dielectric permittivities of lamellar VO_2/Au metamaterial in the directions parallel (\parallel) and perpendicular (\perp) to the sample's surface, when VO_2 is in the semiconductor phase at 20 °C (a) and in the metallic phase at 84 °C (b).

The reflectance spectra of the VO_2/Au metamaterial were collected in p polarization, below and above the phase transition temperature at three incidence angles equal to 15°, 45° and 65°. The spectra measured at 45° are depicted in Fig. 6(a). The wavy pattern in the spectra is due to the parasitic interference effect. Alternatively, the corresponding reflectance spectra have been modeled by substituting the effective dielectric permittivities (Eq. 1) to the known formulas from Ref. 35, Fig. 6(b). The experiment and the calculation are in a fairly good qualitative agreement with each other in a sense that in both cases, the reflectance in the semiconductor (hyperbolic) phase is slightly larger than that in the metallic phase. The qualitatively similar pattern has been observed at the incidence angles equal to 15° and 65°.

The angular dependence of the metamaterial's reflectance was measured at $\lambda = 1200$ nm and $\lambda = 1800$ nm in s and p polarizations, below and above the phase transition temperature, Fig. 6(c). The analogous modeled spectra (calculated as explained above) are depicted in Fig. 6d. One can see that in both theory and experiment (similarly to Figs. 6(a) and 6(b)), the reflection in the semiconductor (hyperbolic) phase is slightly larger than that in the metallic phase, see Figs. 6(c) and 6(d). At the same time, in contrary to Figs. 6(a) and 6(b), the experimental reflectance is smaller than the one predicted theoretically. The reason for this disagreement is not fully understood.

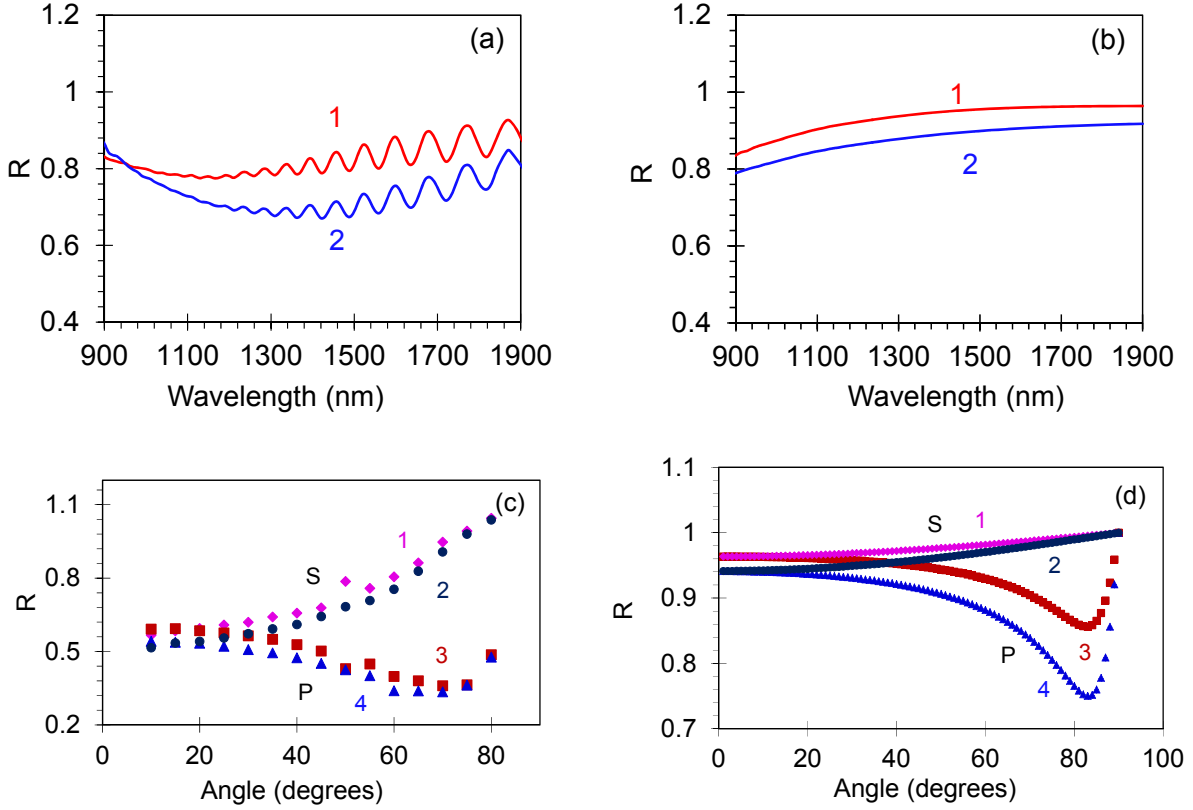


FIG. 6. Reflectance spectra of the VO₂/Au metamaterial, in p polarization at 45° incidence angle, below (trace 1) and above (trace 2) the phase transition: experiment (a) and calculation (b). Angular reflectance profiles of the VO₂/Au metamaterial in s and p polarizations below (traces 1,3) and above (traces 2,4) the phase transition at $\lambda=1800$ nm: experiment (c) and calculation (d).

To summarize, we have fabricated thin VO₂ films and lamellar VO₂/Au metamaterials and studied their electrical and optical properties. Expectedly, VO₂ demonstrated the phase transition from the semiconductor (dielectric) phase to the metallic phase at $\sim 68^\circ\text{C}$. This was evident by (i) dramatic change in the dc electric resistivity, (ii) modification of the reflection and the transmission spectra, and (iii) alteration of dielectric permittivity at optical frequencies, whose real part transformed from positive, like in dielectric to negative, like in metal. The latter behavior governed effective dielectric permittivity of the metamaterial and was responsible for the *optical* phase transition between the hyperbolic and the metallic states at $\lambda > 1000$ nm. The experimentally measured angular and spectral dependences of the metamaterials' reflectance were in a fairly good agreement with the model predictions. The demonstrated optical hyperbolic-to-metallic phase transition is a novel physical phenomenon having a potential to advance the control of light-matter interaction.

Acknowledgements

The work was partly supported by the NSF PREM grant DMR 1205457, ARO grant W911NF-14-1-0639 and AFOSR grant FA9550-14-1-0221. The Lincoln Laboratory portion of this work was sponsored by the Assistant Secretary of Defense for Research & Engineering under Air Force Contract No. FA8721-05-C-0002. Opinions, interpretations, conclusions, and

recommendations are those of the authors and are not necessarily endorsed by the United States Government.

References

- ¹V. M. Shalaev and W. Cai, *Optical Metamaterials: Fundamentals and Applications* (Springer, New York, 2010).
- ²D. R. Smith, and R. Liu, *Metamaterials: Theory, Design, and Applications* (Springer, New York, 2010).
- ³N. Engheta and R. W. Ziolkowski, *Metamaterials: Physics and Engineering Explorations* (John Wiley & Sons, 2006).
- ⁴M. A. Noginov and V. A. Podolskiy , *Tutorials in Metamaterials*. (CRC press, 2011).
- ⁵V. G. Veselago, Sov. Phys. USPEKHI **10**, 509 (1968).
- ⁶V. M. Shalaev, W. Cai, U. K. Chettiar, H. K. Yuan, A. K. Sarychev, V. P. Drachev, and A. V. Kildishev, Opt. Lett **30**, 3356-3358 (2005).
- ⁷R. A. Shelby, D. R Smith, and S. Schultz, Science **292**, 77-79 (2001).
- ⁸J. B. Pendry, Phys. Rev. Lett. **85**, 3966-3969 (2000).
- ⁹N. Fang and X. Zhang, Appl. Phys. Lett. **82**, 161-163 (2003).
- ¹⁰D. Schurig, J. J. Mock, B. J. Justice, S. A. Cummer, J. B. Pendry, A. F. Starr, and D. R. Smith, Science **314**, 977-980 (2006).
- ¹¹N. Engheta, Science **317**, 1698-1702 (2007).
- ¹²P. A. Belov, R. Marques, S. I. Maslovski, I. S. Nefedov, M. Silveirinha, C. R. Simovski and S. A. Tretyakov, Phys. Rev. B **67**, 113103 (2003).
- ¹³D. R. Smith, and D. Schurig, Phys. Rev. Lett. **90**, 077405 (2003).
- ¹⁴A. Salandrino, and N. Engheta, Phys. Rev. B **74**, 075103 (2006).
- ¹⁵Z. Jacob, L. V. Alekseyev, and E. E. Narimanov, Opt. Express **14**, 8247-8256 (2006).
- ¹⁶Z. Jacob, I. I. Smolyaninov and E. E. Narimanov, Appl. Phys. Lett. **100**, 181105 (2012).
- ¹⁷E. E. Narimanov, H. Li, Y. A. Barnakov, T. U. Tumkur, and M. A. Noginov Opt. Express **21**, 14956-14961 (2013).
- ¹⁸M. A. Noginov, H. Li, Y. A. Barnakov, D. Dryden, G. Nataraj, G. Zhu and E. E. Narimanov, Opt. Lett. **35**, 1863-1865 (2010).^{18a} T. Tumkur, G. Zhu, P. Black, Y. A. Barnakov, C. E. Bonner and M. A. Noginov, Appl. Phys. Lett. **99**, 151115 (2011).
- ¹⁹Z. Jacob, J. Kim, G. V. Naik, A. Boltasseva, E. E. Narimanov, and V. M. Shalaev, Appl. Phys. B **100**, 215 (2010).
- ²⁰H. N. Krishnamoorthy, Z. Jacob, E. E. Narimanov, I. Kretzschmar and V. M. Menon Science **336**, 205-209 (2012).
- ²¹L. Gu, T. U. Tumkur, G. Zhu and M. A. Noginov, Sci.Rep. **4**, 7327 (2014).^{21a} L. Gu, T. U. Tumkur, G. Zhu, and M. A. Noginov, Sci. Rep. **4**, 4969 (2014).
- ²²Z. Yang, C. Ko, and S. Ramanathan, Ann. Rev. Mater. Res. **41**, 337-367 (2011).
- ²³F. J. Morin, Phys. Rev. Lett. **3**, 34 (1959).
- ²⁴A. Cavalleri, C. Tóth, C. W. Siders, J. A. Squier, F. Ráksi, P. Forget and J. C. Kieffer, Phys. Rev. Lett. **87**, 237401 (2001).
- ²⁵M. A. Kats, D. Sharma, J. Lin, P. Genevet, R. Blanchard, Z. Yang, M. M. Qazilbash, D. N. Basov, S. Ramanathan, and F. Capasso, Appl. Phys. Lett. **101**, 221101 (2012).
- ²⁶D. W. Ferrara, J. Nag, E. R. MacQuarrie, A. B. Kaye and R. F. Haglund Jr. Nano Lett. **13**, 4169-4175 (2013).

- ²⁷T. Driscoll, H. T. Kim, B. G. Chae, B. J. Kim, Y. W. Lee, N. M. Jokerst, S. Patil, D. R. Smith, M. Di Ventra and D. N. Basov, *Science* **325**, 1518-1521 (2009).
- ²⁸M. J. Dicken, K. Aydin, I. M. Pryce, L. A. Sweatlock, E. M. Boyd, S. Walavalkar, J. Ma, and H. A. Atwater, *Opt. Express* **17**, 18330-18339, 2009.
- ²⁹H. N. Krishnamoorthy, Y. Zhou, S. Ramanathan, E. E. Narimanov and V. M. Menon, *Appl. Phys. Lett.* **104**, 121101 (2014).
- ³⁰Y. Xiong, Q. Y. Wen, Z. Chen, W. Tian, T. L. Wen, Y. L. Jing, Q. H. Yang, and H. W. Zhang, *J. Phys. D: Appl. Phys.* **47**, 455304 (2014).
- ³¹G. E. Jellison and F. A. Modine, *Appl. Phys. Lett.* **69**, 371–373 (1996).
- ³²G. Xu, Y. Chen, M. Tazawa, and P. Jin, *J. Phys. Chem. B* **110**, 2051-2056 (2006).
- ³³S. M. Rytov, *Sov. Phys. JETP* **2**, 466-475 (1956).
- ³⁴J. E. Sipe and R. W. Boyd, *Optical Properties of Nanostructured Random Media*, V. M. Shalaev, ed. (Springer, 2002).
- ³⁵M. A. Noginov, Yu. A. Barnakov, G. Zhu, T. Tumkur, H. Li, and E. E. Narimanov, *Appl. Phys. Lett.* **94**, 151105 (2009).